Associations between histogram analysis parameters derived from morphological sequences and histopathological tissue alterations in myositis and other myopathies: a preliminary study

H.-J. Meyer[1], I. Schneider[2], A. Emmer[2], M. Kornhuber[2], A. Surov[3]

[1]Department of Diagnostic and Interventional Radiology, University of Leipzig, Germany;
[2]Department of Neurology, Martin-Luther-University Halle-Wittenberg, Halle (Saale), Germany;
[3]Department of Radiology and Nuclear Medicine, University of Magdeburg, Germany.

Abstract

Objective

Magnetic resonance imaging (MRI) is a cornerstone in diagnosis of myopathies. Recently, imaging techniques, such as histogram analysis are used to obtain novel imaging biomarkers. The present study sought to elucidate possible associations between histopathology derived from muscle biopsies and histogram parameters derived from clinical MRI in myositis and other myopathies.

Methods

20 patients with myopathies were included in this retrospective study. MRI was performed using a 1.5T MRI scanner including T2- and T1- weighted images. The histogram parameters of the MRI sequences were obtained of the biopsied muscle. The histopathology analysis included the scoring systems proposed by Tateyama et al., Fanin et al., Allenbach et al., and immunohistochemical stainings for MHC-I, CD68, CD8 and CD4.

Results

Entropy derived from T2-weighted images showed strong positive associations with the inflammation scores (r=0.71, p=0.0005 with Allenbach et al score and r=0.68, p=0.001 with Tateyama score). Furthermore, there were strong associations between entropy derived from T2-weighted images with MHC-I staining (r=0.67, p=0.022), with the amount of CD20 cells (r=0.70, p=0.022), with the amount of CD4 positive cells (r=0.78, p=0.0075) and with the amount of CD8 positive cells (r=0.79, p=0.004). Other parameters showed no associations with the investigated histopathology features.

Conclusion

Entropy derived from T2-weighted images showed strong associaitions with inflammation scores and with the sole amount of immune cells in myopathies. These results need to be confirmed by clinical studies, whether it is also related to clinical performance or can predict treatment response.

Key words

magnetic resonance imaging, myositis, myopathy, histogram analysis

Hans-Jonas Meyer, MD
Ilka Schneider, MD
Alexander Emmer, MD
Malte Kornhuber, MD
Alexey Surov, MD

Please address correspondence to:
Hans-Jonas Meyer,
Department of Diagnostic and Interventional Radiology,
University of Leipzig,
Liebigstraße 20,
04103 Leipzig, Germany.
E-mail:
hans-jonas.meyer@medizin.uni-leipzig.de

Received on February 25, 2020; accepted in revised form on April 17, 2020.

Competing interests: none declared.

Introduction

Autoimmune myositis and myopathy are a heterogeneous group of unknown aetiology, which comprises several entities, including inflammatory entities with more acute oedematous behaviour or, *e.g.* dystrophic entities with more degenerative behaviour and muscle fibre dysfunction (1-5).

The diagnostic approach is multimodal consisting of clinical examination, serological parameters, needle electromyography, and histopathology obtained via muscle biopsy (1).

Magnetic resonance imaging (MRI) is a clinically used imaging modality to detect atrophy, muscle oedema and/or myofasciitis. (1, 6). It is established as the most important imaging modality due to its excellent soft tissue contrast.

Currently, MR images are not only used qualitatively, but can also quantitatively be analysed with various approaches (7). One basic technique is histogram analysis, which issues every voxel of a defined region of the MRI into a histogram (7). Typical derived parameters are percentiles, median, mode, skewness, kurtosis and entropy (7).

Previously, some preliminary studies, predominantly on the field of oncologic imaging, provided data that histogram parameters derived from MRI are capable to reflect different microstructure characteristics of tumours, such as cellularity and proliferation potential (8-10). Furthermore, histogram analysis parameters were able to predict treatment response in longitudinal analyses in several malignancies (8-10). So, it was shown that even morphological sequences can reflect tissue features, comprising proliferation potential, cellularity and nucleic sizes in several malignant tumours (8-11).

Presumably, this imaging analysis can also reflect microstructure in muscle disorders and may aid in treatment response evaluation. In fact, some investigations confirmed this hypothesis. For example, it was shown that histogram parameters derived from diffusion-weighted imaging can reflect cellularity parameters in muscle lymphomas (12). Furthermore, in myositis, kurtosis derived from diffusion-weighted imaging was associated with C-reactive protein serum level (13).

However, it is unclear, whether morphological sequences quantified with this approach can also reflect tissue features in myopathies.

Therefore, the purpose of this study was to elucidate possible associations between histogram analysis parameters derived from morphological sequences and histopathological features in myopathy patients using clinical routine MRI and muscle biopsies.

Methods

This retrospective study was approved by the institutional ethic committee (Martin-Luther university of Halle-Wittenberg) and informed consent was waived.

One hundred and six patients with different muscle disorders were investigated by MRI in our department during the time period from 2007 to 2016. Patients were included in this study if they fulfilled the following inclusion criteria:

- muscle disorder confirmed by histopathology;
- patients investigated by clinical MRI including the same T1 and T2-weighted images;
- available histopathological specimens obtained from the same region as the MRI.

Altogether, 20 patients (8 women, 40.0%) with a mean age 51.4±19.0 years yielded the inclusion criteria.

The diagnoses were as follows: undifferentiated myopathy (n=5, 25.0%), overlap myositis (n=5, 25.0%), limb girdle muscle dystrophy (n=3, 15.0%), Inclusion body myositis (n=3, 15.0%), Morbus Pompe (n=1, 5.0%), Anoctamin 5 mutation-related myopathy (n=1, 5.0%), Matrin 3-related muscle disease (n=1, 5.0%), necrotising myositis (n=1, 5.0%) (1, 3, 5).

MRI

MRI of the thigh and lower leg was performed using a 1.5-T scanner (Magnetom Vision Sonata Upgrade, Siemens, Germany). MRI protocol included T2-weighted fat-suppressed short tau inversion recovery (STIR) images (TR 5490 ms, TE 80 ms, flip angle 150°, slice thickness 10 mm),

T1-weighted spin-echo (SE) images without administration of contrast medium (TR 474 ms, TE 11 ms, flip angle 150°, slice thickness 10 mm).

Imaging analysis

MR images were transferred in DICOM format and processed offline with custom-made Matlab-based application (The Mathworks, Natick, MA). Polygonal regions of interest (ROI) were manually drawn along the contours of the muscle, in which the muscle biopsy was obtained. The ROIs were simultaneously placed on T2- and T1-weighted images. All measures were performed by one radiologist blinded to the histopathology results (A.S., 16 years of general radiological experience). The following histogram parameters were calculated: mean, max, min, median, mode, percentiles: 10th, 25th, 75th and 90th, kurtosis, skewness and entropy, as reported previously (8-10). These parameters were each derived from T2- and native T1-weighted images. A patient for illustration purposes is shown in Figure 1.

Muscle biopsies and histological evaluation

The open muscle biopsies were taken of the patients as part of the routine clinical work up after written consent of all patients. The following muscles were biopsied: Vastus lateralis (n=9, 45%), biceps femoris (n=7, 35%), tibialis anterior (n=3, 15%), and adductor magnus (n=1, 5%).

All biopsies were fresh frozen for routine histology and immunohistochemistry. The biopsies were retrospectively examined in a blinded manner to the imaging and clinical report by an experienced neurologist (I.S.) and different grading was applied for inflammation and dystrophic remodelling.

1. Severity of inflammation in each muscle was graded according to Allenbach *et al*. with grading as follows: grade 1: involvement of a single muscle fibre or <5 muscle fibres; grade 2: a lesion involving 5 to 30 muscle fibres; grade 3: a lesion involving a muscle fasciculus; grade 4: diffuse, extensive lesions (14). When multiple lesions with the same grade were found in a single muscle block, 0.5 points were added to the grade.

2. The scoring system published by Tateyama *et al*. was used with separate grading of inflammation, necrosis and regeneration (15)**.** The extent of mononuclear cell infiltration (mononuclear cell infiltration score) was graded:

grade 0: none or slight; grade 1: one focus of mononuclear cell infiltration; grade 2: more than one focus of mononuclear cell infiltration; and grade 3: diffuse mononuclear cell infiltration.

Muscle fibre necrosis and regeneration (necrosis/regeneration score) were graded as follows: grade 0: none; grade 1:1% or less of muscle fibres showing necrosis or regeneration; grade 2: more than 1% and no more than 10% of muscle fibres showing necrosis or regeneration; and grade 3: more than 10% of muscle fibres showing necrosis or regeneration. The total histological score was calculated for each patient by adding the mononuclear cell infiltration and the necrosis/regeneration scores.

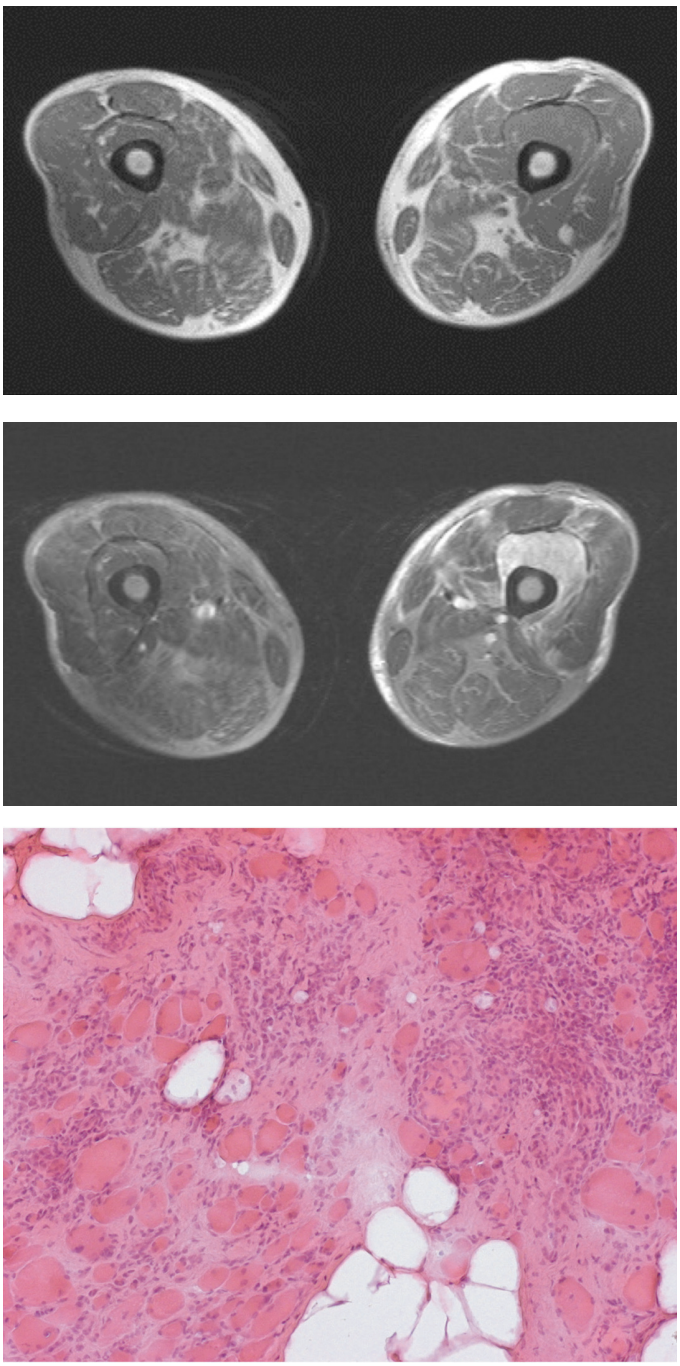

Fig. 1. An illustrative example of a patient in the patient sample with unclear myopathy.

A: Axial T1-weighted image of the upper thigh.
Swelling of the left femoris rectus muscle of the quadriceps femoris muscle can be appreciated.

B. Axial T2-weighted image with fat-suppressed short tau inversion recovery. The left femoris rectus muscle is hyperintense compared to adjacent muscles consistent with oedematous tissue alterations.
Slight movement artefacts are seen.

C: Corresponding histopathology specimen of the muscle haematoxylin-eosin stained in a with low magnification.
Severe infiltration of immune cells can be appreciated.
The score results for this patient are 1 point for Fanin, 0 point for Allenbach, 1 point for Tateyama sum score.

Finally, a 4-point histopathological scale based on the dystrophic changes (histology severity score, HHS), according to Fanin *et al*. was used (16). HSS grade was as follows: grade 1: mild (slight increase in fibre size variability, absent or mild regeneration and degeneration, absent or mild fibrosis); grade 2 moderate (moderate increase in variability of fibre size, variable degeneration and regeneration, moderate or severe fibrosis); grade 3 severe (marked increase in variability of fibre size, variable degeneration and regeneration, moderate or severe fibrosis; and grade 4 advanced (huge increase in variability of fibre size, variable degeneration and regeneration, severe fibrosis).

Routinely used immunohistochemistry included staining for Major histocompatibility complex (MHC)-I, CD68, CD8 and CD4. The number of stained cells per high power field was evaluated. Immunhistochemical analysis was available for 11 patients (55.0% of all patients).

Statistical analysis

Statistical analysis and graphics creation were performed using GraphPad Prism 5 (GraphPad Software, La Jolla, CA, USA). Collected data were evaluated by means of descriptive statistics (absolute and relative frequencies). Spearman's correlation coefficient (p) was used to analyse associations between investigated parameters. In discrimination analysis of subgroups Mann-Whitney test was used. In all instances, p-values <0.05 were taken to indicate statistical significance.

Results

Correlations with histopathology scores

For the dystrophy score (HSS, Fanin *et al*.) one patient had 4 points (5.0%), 2 patients had 3 points (10.0%) 8 patients had 2 points (40.0%) and 9 patients had 1 point (45.5%). There were no significant correlations with the investigated histogram parameters. There was only a statistical tendency for entropy derived from T2-weighted images to correlate with the HSS score (r=0.41, p=0.069).

For the inflammation score, Allenbach 4 points was identified in 2 patients (10.0%), 1.5 points in 3 patients (15.0%), 1 point in 1 patients (5.0%) and 0 points in 14 patients (70.0%).

There was a positive correlation between the Allenbach score and entropy derived from T2-weighted images (r=0.71, p=0.0005). All other parameters were not associated with the score. Moreover, the patients with a score of 0 points had significantly lower entropy values derived from T2-weighted images compared to patients with a score 1 to 4 (mean 3.69±0.35 *vs*. 4.31±0.33, p=0.0044, Fig. 2).

Tateyama 6 points were identified in 2 patients (10.0%), 4 points in 2 patients (10.0%), 3 points in one patient (5.0%), 2 points in 2 patients (10.0%), and 1 point in 5 patients (20.0%), 0 points were identified in 8 patients (40.0%).

A positive correlation was identified between entropy derived from T2-weighted images and the Tateyama score (r=0.68, p=0.001), all other parameters were not associated with the score. The entropy parameter derived from T2-weighted images was also significant lower in the 0-point group compared with the patient group with 1 to 6 points (3.63±0.37 *vs*. 4.04±0.43, p=0.0027, Fig. 3).

Correlations between imaging findings and results of immunhistochemical analysis

Regarding MHC I-staining, 2 patients had 3 points (18.2%), one patient had 2 points (9.1%), 5 patients had 1 point (45.5%) and 3 patients (27.3%) had no visible staining. Entropy derived from T2-weighted images correlated positively with the score of MHC I- staining (r=0.67, p=0.022, Fig. 4). All other parameters showed no association with MHC parameters.

Moreover entropy derived from T2-weighted images showed statistically associations with the amount of CD20 positive cells (r=0.70, p=0.022, Fig. 5A), with the amount of CD4 positive cells (r=0.78, p=0.0075, Fig. 5B) and with the amount of CD8 positive cells (r=0.79, p=0.004, Fig. 5C).

There were no correlations with the amount of CD68 and CD138 positive stained cells and the investigated MRI parameters.

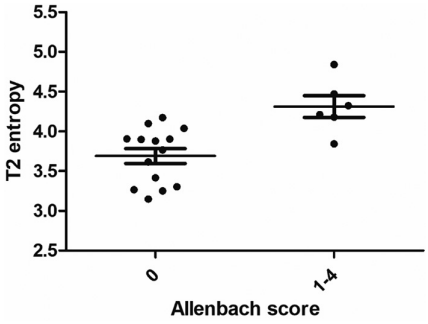

Fig. 2. Box plot graph showing the comparison between patients with Allenbach 0 score and Allenbach 1-4. The patients with a score of 0 points had significant lower entropy values derived from T2-weighted images compared to patients with a score 1 to 4 (mean 3.69±0.35 *vs*. 4.31±0.33, p=0.0044).

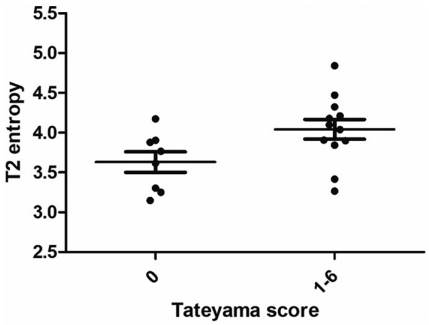

Fig. 3. Box plot graph showing the comparison between patients with Tateyama 0 score and Tateyama 1-6. The entropy parameter derived from T2-weighted images was also significant lower in the 0 point group compared with the patient group with 1 to 6 points (3.63±0.37 *vs*. 4.04±0.43, p=0.0027).

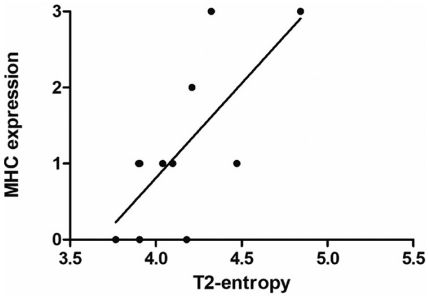

Fig. 4. Correlation analysis between entropy derived from T2-weighted images and MHC I-expression. The Spearman's correlation coefficient is r=0.67, p=0.022.

Discussion

The present study identified strong associations between the parameter entropy derived from routinely used T2-weighted images and underlying histopathology features comprising inflammation scores and the quantified amount of immunity cells in myopathies. No other

Fig. 5A.

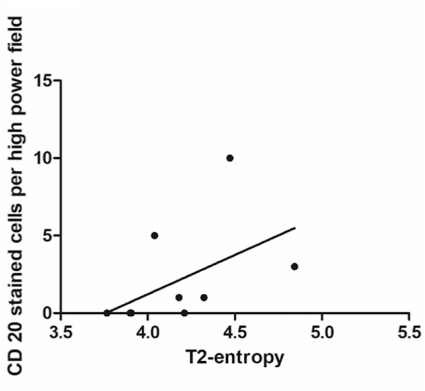

Fig. 5B.

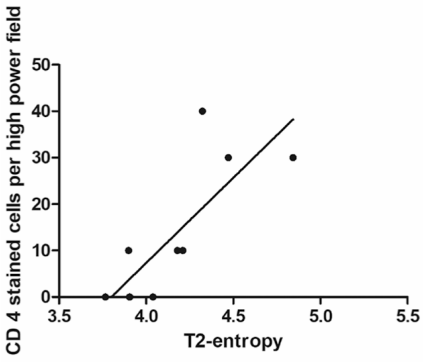

Fig. 5C.

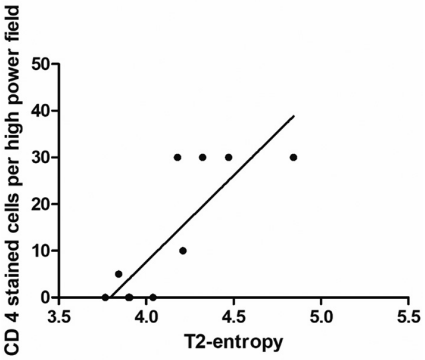

Fig. 5A. Correlation analysis between entropy derived from T2-weighted images and the amount of CD20 positive stained cells. The Spearman's correlation coefficient is r=0.70, p=0.022.

B: Correlation analysis between entropy derived from T2-weighted images and the amount of CD4 positive stained cells. The Spearman's correlation coefficient is r=0.78, p=0.0075.

C: Correlation analysis between entropy derived from T2-weighted images and the amount of CD8 positive stained cells. The Spearman's correlation coefficient is r=0.79, p=0.004.

parameter showed associations with the investigated scores or the immunhistochemical features.

These results strengthen the fact that MRI cannot only be qualitatively assessed by the radiologist to identify diseased muscles but also provide quantitative imaging biomarkers reflecting tissue microstructure in muscle disorders. This is especially of interest since MRI is one of the cornerstones of the diagnostic approach in muscle disorders and routinely acquired with the sequences used in this study (1, 6). So, histogram analysis can be applied without any more effort into the clinical routine (7).

In clinical practice, MRI has been established to be of crucial importance for diagnosing muscle disorders due to its excellent tissue contrast. Thus, the benefit was shown for discrimination purposes of different myopathies, guiding biopsy localisations, and monitoring treatment success (1, 17). Principle imaging findings are muscle oedema, expressed by T2-weighted hyperintense areas. T1-weighted images are mainly used to detect fatty infiltration of the muscles as a chronic disease sign as well as contrast media enhancement, indicating primarily acute inflammatory changes (1, 17).

However, there is still little known about the direct underlying tissue features causing the imaging findings identified by MRI. It was shown that the amount of fatty infiltration of muscles correlates with muscle strength score in inclusion body myositis (18). Recently, a systematic study investigated associations between muscle MRI of the thighs with biopsy pathology in Facioscapulohumeral muscular dystrophy (19), so the oedematous muscles assessed by STIR-sequence were associated with histopathologic confirmed inflammation. Muscles with positive STIR and T1-weighted changes were associated with fibrotic changes (19). These authors used a semiquantitative assessment of muscles with a numeric score. Interestingly however, even MRI-inconspicuous muscles showed in 9/10 biopsies mild to moderate pathologic changes (19), indicating that MRI might not be sensitive enough to identify these mild changes.

The present study used validated histopathology scores with different muscle disorder aspects, the score by Tateyama *et al*. and Allenbach *et al*. are reflective of inflammation (14, 15), whereas Fanin *et al*. score measures the dystrophic changes in muscle disorders (16). One key finding of this study is that entropy derived from T2-weighted images is associated with the inflammation scores by Allenbach *et al*. and Tateyama *et al*. as well as with the quantified number of inflammatory cells of the b cell line. On the contrary, there were no associations with the dystrophic related score of Fanin *et al*.

This histogram parameter entropy quantifies the heterogeneity of the histogram (7). Presumably, the entropy can therefore also reflect the heterogeneity caused inflammations processes in muscle tissue. Interestingly, the heterogeneity of T2-weighted images, mainly influenced by oedematous changes, is indicative of these tissue alterations. It is well known that in the acute inflammation process, first a T2-weighed hyperintense oedema is present, whereas in later stages of the disease fatty dystrophy and atrophy occurs, which are clinically assessed by T1-weighted images (1, 6, 17). This was also shown recently that presence of STIR signal in particular seems more associated with an active myopathic process with ongoing muscle fibre injury and repair with or without associated inflammatory change (19).

There were associations with the amount of CD20, CD4 and CD8 cells. CD20 is an unspecific marker, which every B lymphocyte carries (20). There is some evidence that targeting therapy of CD20 rituximab can help in myositis patients (20). CD4 and CD8 are markers of T lymphocytes (21). Both $CD4^+$ and $CD8^+$ T cells have been described to be present and active in patients with myositis (21). Moreover, predominantly, infiltration of T cells is causing myositis (1). Interestingly, the entropy parameter is associated with MHC I expression, which is mainly expressed by CD8 cells (1). In short, entropy derived from T2-weighted images is directly correlated with the cells causing acute inflammation. The present study can confirm these results that with a quantification of T2-signal alterations associations with inflammation changes can be obtained. Moreover, there might be possible discrimination ability for

patients without a high inflammation score and patients with one.

For oncologic imaging, it was extensively researched that histogram parameters, reflecting the heterogeneity of radiological images, imply predictive power for microstructure in tumours (7-13). This was shown for several tumours, such as glioblastoma, cerebral lymphoma and head and neck squamous cell carcinoma (7-13). Moreover, different histogram parameters derived from different sequences can predict other tissue factors. For example, entropy was especially highlighted in some studies. Therefore, it correlated with p53 expression in uterine cervical cancer (22). In neuroendocrine tumours, it was significantly different between well and poor differentiated tumours (23). In muscle lymphomas entropy derived from diffusion-Weighted Imaging was correlated with nucleic areas (12).

There are several limitations of the present study to address. Firstly, it is of retrospective design with possible known inherent bias. However, imaging and histopathology was evaluated blinded and independently to each other to reduce possible bias. There might be selection bias towards more severe suffering patients, which relates to more comprehensive diagnostic work up including MRI and histopathology. Secondly, our patient sample is relatively small. As another concern the patient sample comprises heterogeneous disease entities. Thirdly, albeit the same muscle was investigated with MRI and biopsy, there might be still some local incongruencies, which might have an impact on the results. Fourthly, the immunohistochemical analysis was only available for 11 of the 20 patients. Fifthly, one radiologist performed the MRI measurements. However, as shown by previous investigations, histogram analysis approach had well reproducibility and interobserver agreement in several disorders including muscle disorders (12, 24).

In conclusion, the present study showed that entropy derived from T2-weighted images is strongly associated with inflammation scores and amount of immune cells in muscle diseases. Presumably, this histogram parameter reflects microstructure in muscle disease best and should be evaluated in further studies employing this imaging analysis. This MR parameter can be suggested as a surrogate marker of inflammation in myopathy.

References

1. DALAKAS MC: Inflammatory muscle diseases. *N Engl J Med* 2015; 372: 1734-47.
2. GILBREATH HR, CASTRO D, IANNACCONE ST: Congenital myopathies and muscular dystrophies. *Neurol Clin* 2014; 32: 689-703.
3. FINSTERER J, LÖSCHER WN, WANSCHITZ J *et al*.: Secondary myopathy due to systemic diseases. *Acta Neurol Scand* 2016; 134: 388-402.
4. DALAKAS MC: Pathophysiology of inflammatory and autoimmune myopathies. *Presse Med* 2011; 40: e237-47.
5. TRIPOLI A, MARASCO E, COMETI L *et al*.: One year in review 2019: idiopathic inflammatory myopathies. *Clin Exp Rheumatol* 2020; 38: 1-10.
6. O'CONNELL MJ, POWELL T, BRENNAN D *et al*.: Whole-body MR imaging in the diagnosis of polymyositis. *AJR Am J Roentgenol* 2002; 179: 967-71.
7. JUST N: Improving tumour heterogeneity MRI assessment with histograms. *Br J Cancer* 2014; 111: 2205-13.
8. MEYER HJ, HÖHN A, SUROV A: Histogram analysis of ADC in rectal cancer: associations with different histopathological findings including expression of EGFR, Hif1-alpha, VEGF, p53, PD1, and KI 67. A preliminary study. *Oncotarget* 2018; 9: 18510-7.
9. MEYER HJ, SCHOB S, MÜNCH B *et al*.: Histogram analysis of T1-weighted, T2-weighted, and postcontrast T1-weighted images in primary CNS lymphoma: correlations with histopathological findings-a preliminary study. *Mol Imaging Biol* 2018; 20: 318-23.
10. MEYER HJ, LEIFELS L, HAMERLA G *et al*.: Histogram analysis parameters derived from conventional T1- and T2-weighted images can predict different histopathological features including expression of Ki67, EGFR, VEGF, HIF-1α, and p53 and cell count in head and neck squamous cell carcinoma. *Mol Imaging Biol* 2019, 21: 740-6.
11. CHANG PD, MALONE HR, BOWDEN SG *et al*.: A multiparametric model for mapping cellularity in glioblastoma using radiographically localized biopsies. *AJNR Am J Neuroradiol* 2017; 38: 890-8.
12. MEYER HJ, PAZAITIS N, SUROV A: ADC histogram analysis of muscle lymphoma-correlation with histopathology in a rare entity. *Br J Radiol* 2018; 91: 20180291.
13. MEYER HJ, EMMER A, KORNHUBER M *et al*.: Histogram analysis derived from apparent diffusion coefficient (ADC) is more sensitive to reflect serological parameters in myositis than conventional ADC analysis. *Br J Radiol* 2018; 91: 20170900.
14. ALLENBACH Y, SOLLY S, GREGOIRE S *et al*.: Role of regulatory T cells in a new mouse model of experimental autoimmune myositis. *Am J Pathol* 2009; 174: 989-98.
15. TATEYAMA M, FUJIHARA K, MISU T *et al*.: Clinical values of FDG PET in polymyositis and dermatomyositis syndromes: imaging of skeletal muscle inflammation. *BMJ Open* 2015; 5: e006763.
16. FANIN M, NARDETTO L, NASCIMBENI AC *et al*.: Correlations between clinical severity, genotype and muscle pathology in limb girdle muscular dystrophy type 2A. *J Med Genet* 2007; 44: 609-14.
17. DAY J, PATEL S, LIMAYE V: The role of magnetic resonance imaging techniques in evaluation and management of the idiopathic inflammatory myopathies. *Semin Arthritis Rheum* 2017; 46: 642-9.
18. GUIMARAES JB, ZANOTELI E, LINK TM *et al*.: Sporadic Inclusion Body Myositis: MRI findings and correlation with clinical and functional parameters. *AJR Am J Roentgenol* 2017; 209: 1340-7.
19. WANG LH, FRIEDMAN SD, SHAW D *et al*.: MRI-informed muscle biopsies correlate MRI with pathology and DUX4 target gene expression in FSHD. *Hum Mol Genet* 2019; 28: 476-86.
20. FASANO S, GORDON P, HAJJI R *et al*.: Rituximab in the treatment of inflammatory myopathies: a review. *Rheumatology* (Oxford) 2017; 56: 26-36.
21. MALMSTRÖM V, VENALIS P, ALBRECHT I: T cells in myositis. *Arthritis Res Ther* 2012; 14: 230.
22. SCHOB S, MEYER HJ, PAZAITIS N *et al*.: ADC Histogram analysis of cervical cancer aids detecting lymphatic metastases _ a preliminary study. *Mol Imaging Biol* 2017; 19: 953-62.
23. DE ROBERTIS R, MARIS B, CARDOBI N *et al*.: Can histogram analysis of MR images predict aggressiveness in pancreatic neuroendocrine tumors? *Eur Radiol* 2018; 28: 2582-91.
24. AHLAWAT S, KHANDHERIA P, DEL GRANDE F *et al*.: Interobserver variability of selective region-of-interest measurement protocols for quantitative diffusion weighted imaging in soft tissue masses: Comparison with whole tumor volume measurements. *J Magn Reson Imaging* 2016; 43: 446-54.